



Published in final edited form as:

Neurocrit Care. 2022 April ; 36(2): 404–411. doi:10.1007/s12028-021-01303-3.

Dynamic Intracranial Pressure Waveform Morphology Predicts Ventriculitis

Murad Megjhani, PhD^{1,2}, Kalijah Terilli, BA^{1,2}, Lakshman Kalasapudi, MA³, Justine Chen, MD^{1,4}, John Carlson, BA^{1,2}, Serenity Miller, BS⁵, Neeraj Badjatia, MD, MS³, Peter Hu, PhD⁵, Angela Velazquez, MD¹, David J. Roh, MD^{1,4}, Sachin Agarwal, MD MPH^{1,4}, Jan Claassen, MD^{1,4}, ES. Connolly Jr, MD^{4,6}, Xiao Hu, PhD^{7,8}, Nicholas Morris, MD³, Soojin Park, MD^{1,2,4}

¹Department of Neurology, Columbia University Vagelos College of Physicians and Surgeons, New York, New York, United States of America

²Program for Hospital and Intensive Care Informatics, Department of Neurology, Columbia University Vagelos College of Physicians and Surgeons, New York, New York, United States of America

³Department of Neurology, Program in Trauma, University of Maryland School of Medicine

⁴New York Presbyterian Hospital – Columbia University Irving Medical Center, New York, New York, United States of America

⁵Department of Anesthesia, Program in Trauma, University of Maryland School of Medicine

⁶Department of Neurosurgery, Columbia University, New York, New York, United States of America

⁷School of Nursing, Duke University, Durham, North Carolina, United States of America

⁸Departments of Electrical and Computer Engineering, Biostatistics and Bioinformatics, Surgery, Neurology, Duke University, Durham, North Carolina, United States of America

Abstract

Objective: Intracranial pressure waveform morphology reflects compliance, which can be decreased by ventriculitis. We investigated whether morphologic analysis of intracranial pressure dynamics predicts the onset of ventriculitis.

Methods: Ventriculitis was defined as culture or Gram-stain positive cerebrospinal fluid warranting treatment. We developed a pipeline to automatically isolate segments of intracranial pressure waveforms from extraventricular catheters, extract dominant pulses, and obtain morphologically similar groupings. We utilized a previously validated clinician-supervised active learning paradigm to identify meta-clusters of triphasic, single-peak, and artifactual peaks. Meta-cluster distributions were concatenated with temperature and routine blood laboratory values to create feature vectors. A L2-regularized logistic regression classifier was trained to distinguish

[†]Corresponding author: Soojin Park, 177 Fort Washington Ave, 8 Milstein – 300 Center, spark@columbia.edu, (212) 305-7236.

⁶Disclosures:

Data Collection (KT, LK, JC, JC, SM, NB, PH, DJR, SA, JC, ESC, NM), Analysis (MM, SP, KT), Writing (MM, SP, KT), Editing (All).

patients with ventriculitis from matched controls and the discriminative performance using area under receiver operating characteristic curve with bootstrapping cross-validation was reported.

Results: Fifty-eight patients were included for analysis. Twenty-seven patients with ventriculitis from two centers were identified. Thirty-one patients with catheters but without ventriculitis were selected as matched controls based on age, gender, and primary diagnosis. There were 1590 hours of segmented data including 396,130 dominant pulses in ventriculitis patients and 557,435 pulses in patients without ventriculitis. There were significant differences in meta-cluster distribution comparing before culture-positivity vs during culture-positivity ($p < 0.001$) and after culture-positivity ($p < 0.001$). The classifier demonstrated good discrimination with median area under receiver operating characteristic 0.70 [IQR 0.55–0.80]. There were 1.5 true alerts (ventriculitis detected) for every false alert.

Conclusion: Intracranial pressure waveform morphology analysis can classify ventriculitis without CSF sampling.

Keywords

Neurocritical care; External Ventricular Drainage; Ventriculitis; ICP waveform; Clustering; Machine Learning

2. Introduction

37,000 patients a year receive an external ventricular drain (EVD) in the setting of acute hydrocephalus in the US, generating in-hospital charges of \$151,672 per patient, or \$5.6 billion dollars a year¹. Up to 22% of patients with EVDs develop ventriculitis². Diagnosis of ventriculitis demands antibiotic treatment and can delay permanent shunt placement. Risk of ventriculitis increases after 9.5 days with EVD in subarachnoid and intracerebral hemorrhage^{3–5}. Risk factors include craniotomy, EVD duration, frequency of cerebrospinal fluid (CSF) sampling, presence of intraventricular hemorrhage (IVH), superficial surgical site infections, CSF leakage, and insertion technique^{6, 7}. EVD-related ventriculitis is associated with significant morbidity and mortality^{8–10}. Severe disturbances in the CSF composition of patients with IVH limit the value of routine CSF analysis for prediction. Diagnosis of ventriculitis¹¹ via the act of CSF retrieval itself contributes to the risk of infection. A less invasive tool for early detection of ventriculitis not reliant on frequent CSF collection would be an advance in the management of patients with EVDs. There are no studies quantifying the ICP waveform dynamics for diagnosing ventriculitis.

Ventriculitis is associated with an inflammation of the ependymal lining of the cerebral ventricles, affecting its functional component of cerebrospinal fluid (CSF) absorption directly into intercellular spaces¹². Disruption of CSF absorption is mechanically reflected in reduced compliance of the brain parenchyma^{13, 14} and measurable in characteristics of intracranial pressure (ICP)¹⁵.

As shown in previous work, ICP waveform morphology dynamics change characteristically up to one day prior to clinical recognition of ventriculitis¹⁶. Our hypothesis is that there is a temporal quantitative signal in ICP waveform reflective of intracranial dynamics that can be translated into a machine learning model to detect ventriculitis.

3. SUBJECT/MATERIALS AND METHODS

3.1. Outcome definition (Ventriculitis Definition)

The clinical diagnosis of ventriculitis is imprecise^{2, 17, 18}, but still demands antibiotic treatment and delay of permanent shunt placement. For the purpose of having a reproducible defined outcome in our study, ventriculitis was defined as obligate culture or Gram-stain positivity that warranted antibiotic treatment.

3.2. Study Population

At Columbia University Irving Medical Center (CUIMC), patients with EVD were identified from a prospective outcomes study of subarachnoid and intracerebral hemorrhage from 2009 to 2019. Ventriculitis patients were identified and matched to control patients based on placement of EVD, age, gender, and primary diagnosis.

At University of Maryland (UMD), patients with EVD and treated ventriculitis patients were identified from a clinical electronic medical record between 2015 and 2019. These patients were matched to control patients based on placement of EVD, age, gender, and primary diagnosis.

3.3. Patient consent

The study was approved by the Institutional Review Boards at the respective centers. In CUIMC, written informed consent was obtained from the patient or a surrogate. In UMD, an exemption for consent was granted because data was deidentified, data was retrospectively analyzed, and no outpatient follow up was sought.

3.4. Monitoring and Data Acquisition

At Columbia, acute hydrocephalus was treated and ICP was monitored using the Integra[®] External Drainage and Monitoring System with antibiotic impregnated Medtronic[®] VentriClear II[®] ventricular drainage catheter or non-antibiotic impregnated Medtronic[®] large translucent ventricular catheter. EVDs were placed following cefazolin prophylaxis for symptomatic hydrocephalus. In settings of significant intraventricular blood, an acute care clinical decision would call for non-antibiotic coated trauma EVD catheters. CSF was sampled three times a week by protocol, and further based on clinical suspicion in the work-up of fever or unexplained alterations in mental status. Physiologic data for the duration of the intensive care unit stay was acquired using a high-resolution acquisition system. From 2009 to 2013, BedmasterEX (Excel Medical Electronics Inc., Jupiter, FL, USA) was used to acquire physiologic data from General Electric Solar 8000i monitors (Port Washington, NY, USA) at 240 samples per second. From 2014 to 2019, ICM+ (Cambridge, UK) was used to acquire physiologic data from Philips Intellivue MP70 monitors (Amsterdam, The Netherlands) at 125 samples per second.

At University of Maryland, ICP was monitored using the Medtronic (Dublin, Ireland) Duet[™] External Drainage and Monitoring System with antibiotic impregnated Codman[®] Bactiseal[®] EVD Catheter Set (Integra Neurosciences). EVDs were placed following cefazolin prophylaxis for symptomatic hydrocephalus. CSF was sampled selectively based

on clinical suspicion in the work-up of fever or unexplained alterations in mental status. BedmasterEX was used to acquire physiologic data for the duration of the intensive care unit stay at 240 samples per second.

BedmasterEx proprietary file format (STP) and ICM+ format (DTA) were converted into the Hierarchical Data Format, version 5 (HDF5; 1997–2018, <http://www.hdfgroup.org/HDF5/>) and MATLAB 2016a (Mathworks, Natick, MA) was utilized for data analysis.

3.5. Data Analysis

The framework of our approach to classify ventriculitis using ICP morphology is summarized in Figure 1 & 2 and described below.

3.5.1. ICP waveform segmentation using wavelet analysis—Common EVD practice in the management of acute hydrocephalus leaves the EVD system unclamped for much of the time. This allows extravascular blood and excess CSF (beyond a pressure threshold) to drain into a collecting system. As a fluid-filled manometer, the EVD only transmits a pressure waveform when the system is clamped; this is done at both centers according to protocol (hourly on an average) by nurses to document the pressure often as any other vital sign. The frequency compositions of the ICP signals (when the system is clamped) and the artifacts (when the system is open) are different. Leveraging this difference, wavelet analysis was used to detect uninterrupted short periods of ICP waveforms from longer periods of non-measurement data¹⁹. Further details are provided in Appendix A.

3.5.2. Dominant Pulse Extraction—A validated technique, morphological clustering analysis of ICP pulse (MOCAIP)²⁰, was used to extract dominant pulses and allow quantitative comparison between pulses. Dominant pulse extraction consists of three components to detect and characterize waveforms. The first step was identification of ICP pulses using QRS complexes in the electrocardiogram (ECG). The second step grouped individual ICP pulses into morphologically similar clusters in short time segments (6 seconds) and applied an averaging and cross-correlation process to extract a representative “dominant” pulse. In the third step of MOCAIP, all dominant pulses would be compared against an expert-validated reference library of non-artifactual pulses. However, for the purposes of this study this third step was eliminated as selection bias could be introduced against certain pulses at the extreme of decreased intracranial compliance. This would erroneously remove physiologically valid single-peak pulses. Artifactual waveform detection and removal is instead addressed later in analysis using a semi-supervised active learning method. ICP waveform segmentation and dominant pulse extraction were performed in MATLAB 2016a (Mathworks, Natick, MA).

3.5.3. Clustering Analysis—After the extraction of dominant pulses, dynamic time warping (DTW)^{21, 22} and hierarchical k -means ($k = 20$) were applied to identify waveforms with similar morphology. DTW is a method for measuring similarity between two temporal sequences that may vary in speed; this allowed for comparison of ICP waveforms between patients with varying heart rate. Clusters were further split if the mean within-cluster

distance (measuring the closeness of waveforms to centroid of the cluster) times the variance (measuring the dispersion of waveforms in the cluster group around the centroid) was greater than a threshold of 1, or if the number of waveforms within the cluster group was >1000. The resulting leaf nodes were then used to determine meta-clusters.

Meta-clusters were identified using an active-learning approach with clinician input (Appendix B–D)²³. Distribution of the meta-clusters before, during, and after periods of culture-positive ventriculitis and in matched control subjects were compared using the chi-square test of independence.

3.5.4. Machine Learning Analysis—A machine-learning model was developed to classify ventriculitis, using the meta-clusters, body temperature, and routinely available intensive care laboratory values (i.e. basic metabolic panel, white and red blood cell counts). These laboratory values were considered during feature selection because in experimental sepsis, disturbances of the hypothalamic-pituitary-adrenal axis affect plasma electrolytes (including sodium, potassium, chloride, magnesium)²⁴. The approach was adapted from a Bag of Words (BoW) model, developed for natural language processing^{25, 26}. To construct the BoW feature representation, the occurrences in the ICP data of each of the three meta-clusters, before, during, and after the culture-positivity period were determined for patients with ventriculitis, and for the entire duration of EVD for patients without ventriculitis. These features were then concatenated with median ICP and median, min and max of 12 additional clinical features from blood laboratory values that were universally available for these patients (sodium, potassium, chloride, glucose, calcium, magnesium, HCO₃, blood urea nitrogen (BUN), creatinine, white blood cell (WBC) count, red blood cell (RBC) count) and temperature, resulting in total of 40 features. Data from the two institutions were combined to train a L2-regularized logistic regression classifier for the occurrence of ventriculitis (during vs control). Three-fold cross-validation was performed on 80% of data to tune model parameters and a hold-out set of 20% was used to report the accuracy. This process was repeated for 500 iterations.

The area under the receiver operating characteristic curve (AUROC) and confusion matrix (indicating true positive, true negative, false positive and false negative) was used to describe the performance of the models²⁷. We reported the median [IQR] over 500 iterations. Clustering analysis and machine-learning models were developed using the Python scikit-learn library²⁸.

3.5.5. Data availability—All relevant data are presented within the article and its supporting information files. Additional information can be obtained upon reasonable request to the corresponding author.

4. Results

At CUIMC between June 2009 and June 2019, 118 patients with EVD were diagnosed with clinically-defined ventriculitis that warranted antibiotic treatment. Positive CSF Gram stain or cultures were identified for 18 of these patients (15% of clinical ventriculitis). At UM

between July 2015 to July 2019, 9 patients with EVD were diagnosed with clinically-defined ventriculitis.

Control patients with EVD and similar age, gender and primary diagnosis were identified during this time frame. Both cohorts were combined into a single dataset (27 ventriculitis, 31 control) and characteristics were statistically compared (Table 1, Appendix F). Due to missing ICP data, the number of control patients was greater than the number of ventriculitis patients included in the final analysis.

Patients with ventriculitis had worse GCS at admission, more CSF cultures, fewer antibiotic-coated catheters and multiple EVDs placed. Patients with ventriculitis also had longer lengths of stay in the hospital by a median of four days compared to controls ($p = 0.019$).

1590 hours of segmented data were extracted, and 953,565 dominant ICP pulses were identified. Of those, 396,130 (41.5%) dominant pulses were identified in patients with ventriculitis, with 132,586 (33.5%) dominant pulses before culture-positivity, 144,728 (36.5%) during culture-positivity, and 118,816 (30%) after culture-positivity. A total of 557,435 (58.5 %) dominant pulses were identified in control patients (Figure 3A).

4.1. Cluster Analysis

Using k -means hierarchical clustering, 311 centroid clusters (leaf nodes) were found. An active learning algorithm with clinician input was then used to identify meta-clusters as triphasic, single-peak or artifactual. 35 (11%) leaf nodes were classified as triphasic, 97 (31%) leaf nodes as single-peak and 179 (58%) leaf nodes as artifact (Figure 3B). 32.1% of the dominant pulses were triphasic before culture positivity, when compared to 20.5% during culture positivity. 61.3% of the dominant pulses were single peaks during culture-positivity when compared to 52% before and 55.6% after culture-positivity. The total percentage of single-peak pulses after culture-positivity (55.6%) was similar to that of the control cohort (53.9%) (Figure 3A).

A chi-square test of independence showed that there were significant differences among the distribution of these clusters between during ventriculitis and control groups ($p=0.045$), as well as after ventriculitis and control groups ($p=0.045$) (Figure 3A).

4.2. Model Performances

L2-regularized logistic regression was applied to ascertain the power of ICP-derived measures for classifying ventriculitis. Ventriculitis positivity was classified with a median [IQR] AUROC of 0.70 [0.55–0.80], true positive 0.6 [0.4–0.8], false positive 0.4 [0.2–0.6], false negative 0.33 [0.17–0.5] and true negative 0.67 [0.5–0.83] (Figure 4). In other words, there were 1.5 true alerts (ventriculitis detected) for every false alert. We also performed an ablation analysis with and without the lab values and as expected, our model performed best when we include all the features (Appendix G).

The weights of the classifier indicate the discriminative power of the features in separating the two classes revealing C1 (triphasic morphology), potassium, calcium, magnesium, red blood cell count and temperature to be relevant for classifying ventriculitis (Appendix E).

5. Discussion

In previous work, we discovered significant changes in ICP waveform morphology with ventriculitis, reflective of worsening compliance¹⁶. This difference was seen a day before diagnostic cultures were sent, suggesting ICP morphology has potential as a diagnostic tool. Early antibiotics are a mainstay of infectious disease management; delay of antibiotics in meningitis can adversely impact mortality and neurologic deficits^{29–34}. Sampling CSF daily paradoxically increases the risk of ventriculitis⁸. A model to detect early ventriculitis which bypasses or reduces CSF sampling would be useful for management of these patients.

A machine-learning model derived from ICP morphology features and a few clinical variables (routine laboratory values including complete blood cell and basic metabolic panels and temperature) showed moderately good classification of ventriculitis with an AUROC of 0.70 [IQR 0.55–0.80].

To our knowledge, this is the first study leveraging characteristics of ICP waveform morphology to identify ventriculitis. The finding of differences in ICP morphology with ventriculitis is significant and by comparing to matched controls, confirmed not to be spurious or merely related to EVD duration.

There are some limitations to the translational piece of our study. The definition of ventriculitis used for inclusion was restrictive but unassailable. Unfortunately, this resulted in a model trained on only 58 patients. A model including patients with a broader clinical diagnosis of treated ventriculitis (118 vs 18 in Columbia's cohort) would have increased the numbers greater than six fold, but also introduced significant bias that would potentially reduce generalizability. Efforts will be made instead to continue to accrue more ICP waveform data from patients with culture positive ventriculitis through collaboration. To generalize our findings further, an external or prospective validation will be required. Another limitation of our study is that the usefulness of the model depends on the availability of digitized inputs. Fortunately, informatics in hospitals and critical care is evolving, enabling deployment of models that rely on integrating electronic health record systems and physiologic monitoring systems.

As a product of this study, we have developed a pipeline to: i) identify ICP waveforms automatically from intermittent clamping periods using wavelet analysis, ii) normalize for comparison with dynamic time warping, iii) extract dominant pulses, iv) cluster dominant pulses, v) featurize clusters as “words in a bag” (BoW), vi) train L2-regularized LR model to classify for ventriculitis. Future work will involve prospective application and validation of this method in external and prospective settings.

Supplementary Material

Refer to Web version on PubMed Central for supplementary material.

Acknowledgments

This study was funded by National Institute of Health (NIH), grant number: R21NS113055 (SP) and American Heart Association, grant number 20POST35210653 (MM).

NM reports funding from Accelerated Translational Incubator Pilot Grant through the University of Maryland Baltimore Institute of Clinical and Translational Research unrelated to this study.

References

1. Rosenbaum BP, Vadera S, Kelly ML, Kshetry VR, Weil RJ. Ventriculostomy: Frequency, length of stay and in-hospital mortality in the United States of America, 1988–2010. *Journal of clinical neuroscience : official journal of the Neurosurgical Society of Australasia*. Apr 2014;21(4):623–32. doi:10.1016/j.jocn.2013.09.001 [PubMed: 24630243]
2. Lewis A, Wahlster S, Karinja S, Czeisler BM, Kimberly WT, Lord AS. Ventriculostomy-related infections: The performance of different definitions for diagnosing infection. *Br J Neurosurg*. 2016;30(1):49–56. doi:10.3109/02688697.2015.1080222 [PubMed: 26372297]
3. Kirmani AR, Sarmast AH, Bhat AR. Role of external ventricular drainage in the management of intraventricular hemorrhage; its complications and management. *Surg Neurol Int*. 2015;6:188. doi:10.4103/2152-7806.172533 [PubMed: 26759733]
4. Lewis A, Irvine H, Ogilvy C, Kimberly WT. Predictors for delayed ventriculoperitoneal shunt placement after external ventricular drain removal in patients with subarachnoid hemorrhage. *Br J Neurosurg*. Apr 2015;29(2):219–24. doi:10.3109/02688697.2014.967753 [PubMed: 25299790]
5. Kuo LT, Lu HY, Tsai JC, Tu YK. Prediction of Shunt Dependency After Intracerebral Hemorrhage and Intraventricular Hemorrhage. *Neurocrit Care*. May 22 2018;doi:10.1007/s12028-018-0532-x
6. Busl KM. Nosocomial Infections in the Neurointensive Care Unit. *Neurol Clin*. Nov 2017;35(4):785–807. doi:10.1016/j.ncl.2017.06.012 [PubMed: 28962814]
7. Savin I, Ershova K, Kurdyumova N, et al. Healthcare-associated ventriculitis and meningitis in a neuro-ICU: Incidence and risk factors selected by machine learning approach. *Journal of critical care*. 2018;45:95–104. [PubMed: 29413730]
8. Lozier AP, Sciacca RR, Romagnoli MF, Connolly ES Jr. Ventriculostomy-related infections: a critical review of the literature. *Neurosurgery*. Feb 2008;62 Suppl 2:688–700. doi:10.1227/01.neu.0000316273.35833.7c [PubMed: 18596436]
9. Kitchen WJ, Singh N, Hulme S, Galea J, Patel HC, King AT. External ventricular drain infection: improved technique can reduce infection rates. *Br J Neurosurg*. Oct 2011;25(5):632–5. doi:10.3109/02688697.2011.578770 [PubMed: 21848440]
10. Lyke KE, Obasanjo OO, Williams MA, O'Brien M, Chotani R, Perl TM. Ventriculitis complicating use of intraventricular catheters in adult neurosurgical patients. *Clin Infect Dis*. Dec 15 2001;33(12):2028–33. doi:10.1086/324492 [PubMed: 11712094]
11. Schade RP, Schinkel J, Roelandse FW, et al. Lack of value of routine analysis of cerebrospinal fluid for prediction and diagnosis of external drainage-related bacterial meningitis. *Journal of neurosurgery*. Jan 2006;104(1):101–8. doi:10.3171/jns.2006.104.1.101 [PubMed: 16509153]
12. Sarnat HB. Ependymal reactions to injury. A review. *J Neuropathol Exp Neurol*. Jan 1995;54(1):1–15. doi:10.1097/00005072-199501000-00001 [PubMed: 7815072]
13. Vardakis JC, Tully BJ, Ventikos Y. Multicompartmental poroelasticity as a platform for the integrative modeling of water transport in the brain. *Computer models in biomechanics*. Springer; 2013:305–316.
14. Smillie A, Sobey I, Molnar Z. A hydro-elastic model of hydrocephalus. 2004;
15. Bothwell SW, Janigro D, Patabendige A. Cerebrospinal fluid dynamics and intracranial pressure elevation in neurological diseases. *Fluids Barriers CNS*. Apr 2019;16(1):9. doi:10.1186/s12987-019-0129-6 [PubMed: 30967147]
16. Megjhani M, Terilli K, Kaplan A, et al. Use of Clustering to Investigate Changes in Intracranial Pressure Waveform Morphology in Patients with Ventriculitis. *Acta Neurochir Suppl*. 2021;131:59–62. doi:10.1007/978-3-030-59436-7_13 [PubMed: 33839819]
17. Horan TC, Andrus M, Dudeck MA. CDC/NHSN surveillance definition of health care-associated infection and criteria for specific types of infections in the acute care setting. *American journal of infection control*. 2008;36(5):309–332. [PubMed: 18538699]

18. Czeisler B, Choi HA, Guo K, et al. Comparison between Institutionally-Defined Clinical Criteria and CDC-Criteria for the Diagnosis of Ventriculostomy-Related Infection (P02. 220). AAN Enterprises; 2012.
19. Strang G, Nguyen T. Wavelets and filter banks. SIAM; 1996.
20. Hu X, Xu P, Scalzo F, Vespa P, Bergsneider M. Morphological clustering and analysis of continuous intracranial pressure. *IEEE Trans Biomed Eng.* Mar 2009;56(3):696–705. doi:10.1109/tbme.2008.2008636 [PubMed: 19272879]
21. Niennattrakul V, Ratanamahatana CA. On clustering multimedia time series data using k-means and dynamic time warping. *IEEE*; 2007:733–738.
22. Keogh EJ, Pazzani MJ. An enhanced representation of time series which allows fast and accurate classification, clustering and relevance feedback. American Association for Artificial Intelligence Press; 1998:239–241.
23. Megjhani M, Alkhachroum A, Terilli K, et al. An active learning framework for enhancing identification of non-artifactual intracranial pressure waveforms. *Physiol Meas.* Dec 2018;doi:10.1088/1361-6579/aaf979
24. Flierl MA, Rittirsch D, Weckbach S, et al. Disturbances of the hypothalamic-pituitary-adrenal axis and plasma electrolytes during experimental sepsis. *Ann Intensive Care.* Dec 2011;1:53. doi:10.1186/2110-5820-1-53 [PubMed: 22208725]
25. Csurka G, Bray C, Dance C, Fan L. Visual ceteoration with bags of keypoints. Workshop on Statistical Learning in Computer Vision, ECCV. 2004:1–22.
26. Sivic J, Zisserman A. Video Google: a text retrieval approach to object matching in videos. 2003:1470–1477 vol.2.
27. Hanley JA, McNeil BJ. A method of comparing the areas under receiver operating characteristic curves derived from the same cases. *Radiology.* Sep 1983;148(3):839–43. doi:10.1148/radiology.148.3.6878708 [PubMed: 6878708]
28. Pedregosa F, Varoquaux G, Gramfort A, et al. Scikit-learn: Machine learning in Python. *Journal of machine learning research.* 2011;12(Oct):2825–2830.
29. Bodilsen J, Dalager-Pedersen M, Schonheyder HC, Nielsen H. Time to antibiotic therapy and outcome in bacterial meningitis: a Danish population-based cohort study. *BMC Infect Dis.* Aug 9 2016;16:392. doi:10.1186/s12879-016-1711-z [PubMed: 27507415]
30. Koster-Rasmussen R, Korshin A, Meyer CN. Antibiotic treatment delay and outcome in acute bacterial meningitis. *J Infect.* Dec 2008;57(6):449–54. doi:10.1016/j.jinf.2008.09.033 [PubMed: 19000639]
31. Proulx N, Frechette D, Toye B, Chan J, Kravcik S. Delays in the administration of antibiotics are associated with mortality from adult acute bacterial meningitis. *QJM.* Apr 2005;98(4):291–8. doi:10.1093/qjmed/hci047 [PubMed: 15760921]
32. Lepur D, Barsic B. Community-acquired bacterial meningitis in adults: antibiotic timing in disease course and outcome. *Infection.* Jun 2007;35(4):225–31. doi:10.1007/s15010-007-6202-0 [PubMed: 17646915]
33. Auburtin M, Wolff M, Charpentier J, et al. Detrimental role of delayed antibiotic administration and penicillin-nonsusceptible strains in adult intensive care unit patients with pneumococcal meningitis: the PNEUMOREA prospective multicenter study. *Critical care medicine.* Nov 2006;34(11):2758–65. doi:10.1097/01.CCM.0000239434.26669.65 [PubMed: 16915106]
34. Aronin SI, Peduzzi P, Quagliarello VJ. Community-acquired bacterial meningitis: risk stratification for adverse clinical outcome and effect of antibiotic timing. *Ann Intern Med.* Dec 1998;129(11):862–9. doi:10.7326/0003-4819-129-11_part_1-199812010-00004 [PubMed: 9867727]

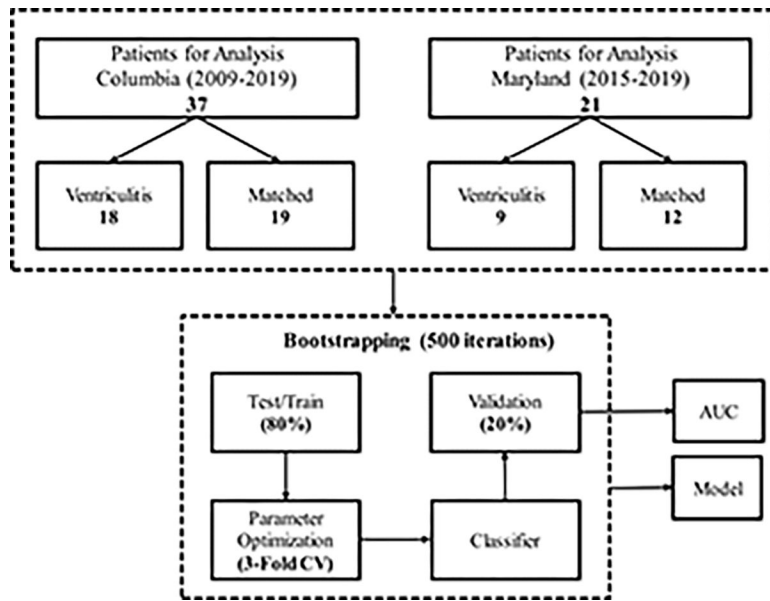


Figure 1:
Overview of the approach.

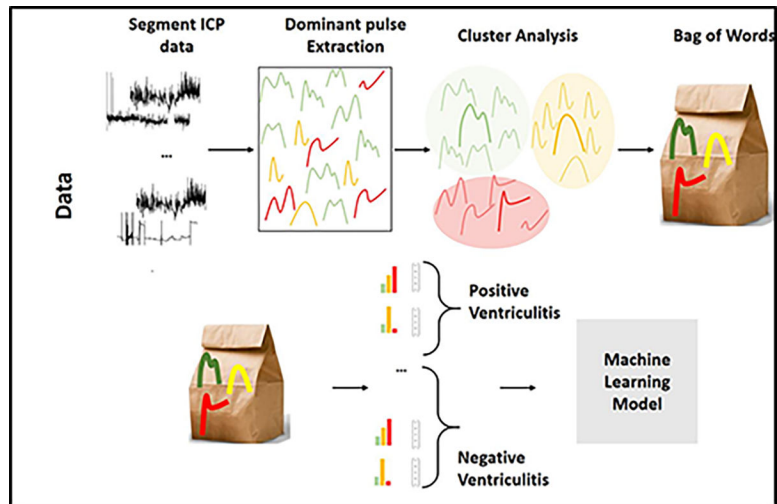


Figure 2: Steps for the bag-of-words (BoW) feature representation and constructing classifiers using BoW features for ventriculitis.

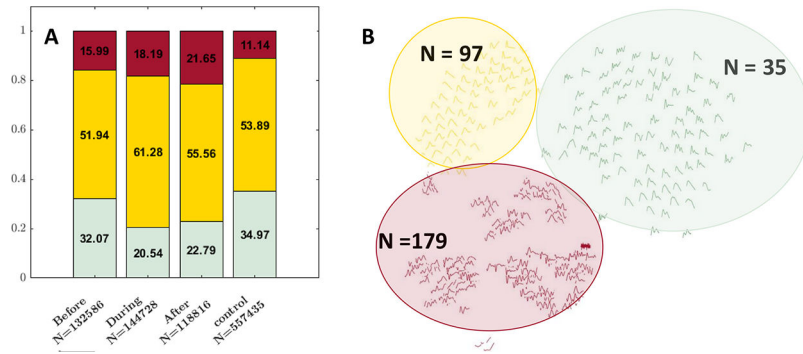


Figure 3: Illustrates the changes in the distribution of the ICP waveforms. (A) Distribution of meta-clusters (green: triphasic; yellow: single-peak; red: artifacts) in control vs before, during, after the culture or Gram-stain positive stage of ventriculitis. (B) Displays 311 leaf nodes, green color indicates triphasic, yellow single-peak and red artifacts.

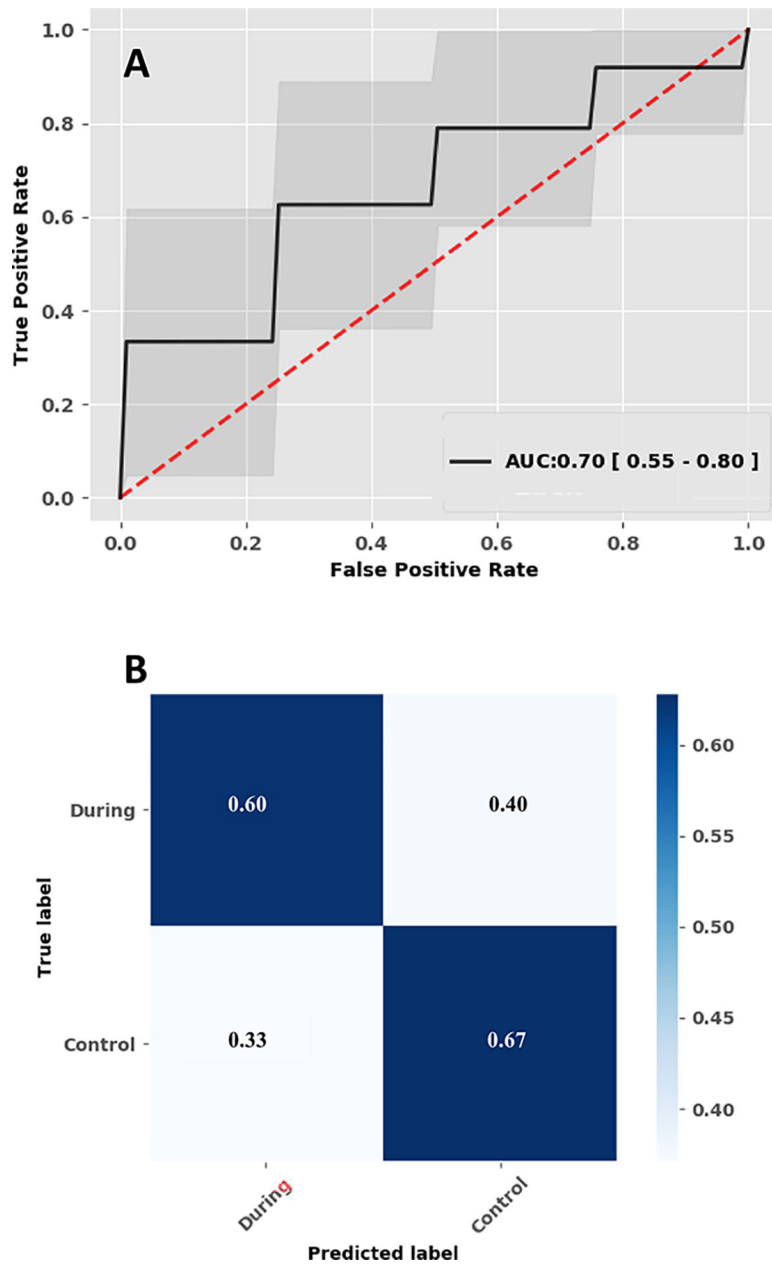


Figure 4: Illustrates the performance of the machine learning model. (A) Performance of the logistic regression model, median Area under the receiver operating characteristic curve. (B) Confusion matrix.

Table 1.

Comparison of patient characteristics

	CUIMC + UMD		<i>p value</i> *
	Ventriculitis n=27	Control n=31	
Age, median (IQR)	64 (49–72)	58 (51–69)	<i>0.488</i>
Female Gender, n (%)	16 (59.3)	20 (64.5)	<i>0.788</i>
Immunosuppressed, n (%)	4 (14.8)	4 (12.9)	<i>1</i>
GCS on Admission, median (IQR)	7 (5–12)	11 (6–15)	<i>0.020</i>
Number of CSF Cultures, median (IQR)	10 (6–16)	3 (2–6)	<i><0.0001</i>
Primary Diagnosis			<i>0.134</i>
ICH, n (%)	8 (29.6)	10 (32.3)	
Brain Tumor, n (%)	1 (3.7)	4 (12.9)	
Other, n (%)	6 (22.2)	1 (3.2)	
SAH, n (%)	12 (44.4)	16 (51.6)	
WFNS, 4 – 5, n (%)	9/12 (75.0)	10/16 (62.5)	
Intraventricular Blood, n (%)	13 (48.1)	17 (54.8)	<i>0.793</i>
Ventilation, n (%)	22 (81.5)	21 (67.7)	<i>0.368</i>
EVD Location			<i>0.133</i>
Right Frontal EVD, n (%)	20 (74.1)	23 (74.2)	
Left Frontal EVD, n (%)	4 (14.8)	8 (25.8)	
Bilateral EVD, n (%)	3 (11.1)	0 (0.0)	
Antibiotic-Coated EVD, n (%)	10 (37.0)	25 (80.6)	<i>0.001</i>
Total EVDs Placed, median (IQR)	1 (1–2)	1 (1–1)	<i>0.002</i>
VP Shunt, n (%)	7 (25.9)	5 (16.1)	<i>0.518</i>
EVD Duration, d, median (IQR)	15 (10–21)	12 (7–18)	<i>0.180</i>
Ventriculitis Duration, d, median (IQR)	7 (4–16)	<i>N/A</i>	
EVD to Ventriculitis, d, median (IQR)	4 (0–8)	<i>N/A</i>	
ICU LOS, d, median (IQR)	20 (15–26)	18 (11–22)	<i>0.117</i>
Hospital LOS, d, median (IQR)	26 (21–52)	22 (15–28)	<i>0.019</i>

	CUIMC + UMD		<i>p value</i> *
	Ventriculitis n=27	Control n=31	
Mortality, n (%)	5 (18.5)	5 (16.1)	<i>1</i>
Discharge Destination			<i>0.349</i>
Home, n (%)	4 (14.8)	7 (22.6)	
Skilled Nursing Facility, n (%)	0 (0.0)	0 (0.0)	
Subacute Rehab, n (%)	11 (40.7)	5 (16.1)	
Rehab, n (%)	2 (7.4)	4 (12.9)	
Acute Rehab, n (%)	5 (18.5)	10 (32.3)	
Hospice, n (%)	2 (7.4)	1 (3.2)	
Deceased, n (%)	3 (11.1)	4 (12.9)	

* considered significant if $p < 0.05$

Author Manuscript

Author Manuscript

Author Manuscript

Author Manuscript